CHARACTERIZATION OF FLUIDS USING OSCILLATORY MEASUREMENTS

Mohammad Reza Mobaraki, Mohammad Ali Adelian

rezaamo1989@gmail.com   ,ma_adelian@yahoo.com

Abstract— Fracturing fluid has a very important role in hydraulic fracturing treatment. Viscosity of hydraulic fracturing fluid affects transporting, suspending, and deposition of proppant, as well as flow back after treatment. It should also be capable of developing the necessary fracture width to accept proppants or to allow deep acid penetration. Compatibility with formation fluids and material has to be taken into account [11].

Rheology of the fracturing fluid is fundamental for hydraulic fracturing design, i.e. prediction of fracture growth and geometry. Accurate measurements and a good understanding of rheological properties of hydraulic fracturing fluids are essential for designing and executing an optimum treatment. Failure in the selection of fracturing fluid will result in unsuccessful treatment in term of reservoir conditions, oil production, and net present value.

Borate cross-linked fluids have been widely used as a fracturing fluid in the oil industry. An experimental study has been conducted to investigate the rheological properties of borate cross-linked fluids and the results are presented in this paper.

Many oscillatory measurements have been conducted to investigate the behaviour of the rheological properties of the fracturing fluid samples under different conditions and the possible relationship among them. Results of the oscillatory measurements of certain borate cross-linked fluids are shown in this paper. It was demonstrated that the linear-viscoelastic limit and flow-point frequency are dependent on temperature.

Keywords— Stimulation, Acid, Hydraulic Fracturing, Matrix acidizing, Polymer Concentration, Time test oscillation, Amplitude sweep, Frequency sweep, Temperature test oscillation.

INTRODUCTION

Reservoir stimulation and artificial lift are the two main activities of the production engineer in the petroleum and related industries. The main purpose of stimulation is to enhance the property value and/or to increase ultimate economic recovery. The stimulation treatments are intended to remedy, or even improve, the natural connection of the wellbore with the reservoir [5].

Materials in this chapter were taken from [27], [6], [5], [4].

Methodology

1.1. Reservoir Justification of Stimulation Treatments

There are two main areas of interest for a stimulation treatment:
1. Wellbore zone and its proximity
2. Rest of a reservoir

Different kinds of stimulation technology are generally used depending on the area of interest:
1. Acid washing
2. Matrix acidizing
3. Acid fracturing
4. Hydraulic fracturing

Stimulation is needed to remove skin zones around the wellbore. The total skin effect is a composite of a number of factors that can be divided into pseudoskin and formation damage as shown in Fig. 1.

Pseudoskin effects are defined as skins that appear due to 1) limited entry; 2) off-centered well; 3) gas blockage; 4) turbulent flow in the vicinity of a well; 5) collapsed tubing; or 6) poor isolation due to poor cementation.

Formation damage is a result of the following failures:

Drilling damage due to drilling mud solid invasion and/or drilling filtrate invasion:

- Cementing damage due to cement slurry invasion
- Perforation damage
- Damage during production due to precipitation of organic/inorganic material, bridging, and blocking
- Damage during stimulation treatment

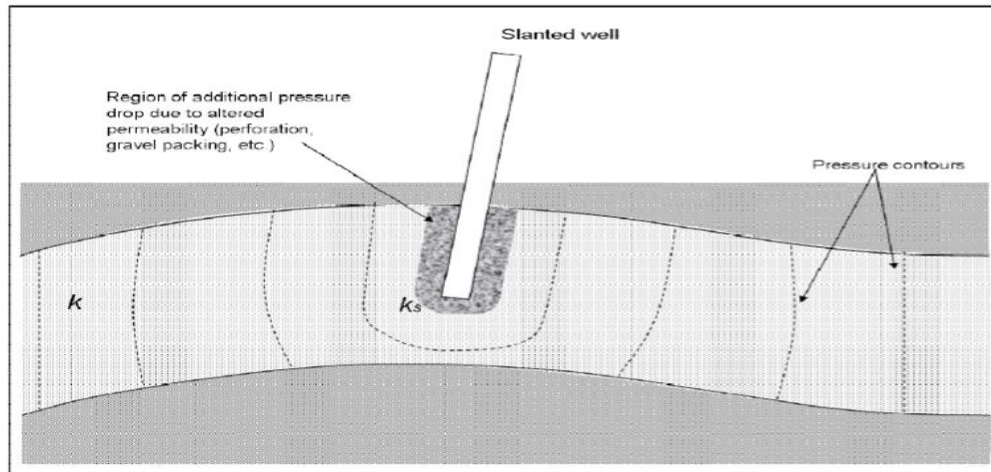Skin analysis has to be performed prior to stimulation treatment.

Figure 1 Skin effect due to converging of flow lines and near wellbore permeability impairment (Zolotukhin et al. 2005)

1.2. Types of Stimulation Treatment:

There are several types of stimulation treatment that can be conducted to remove the skin effect.

Acid washing is a type of stimulation to remove acid soluble scales present in the wellbore or to open perforations. Acid washing is the least expensive of all the near wellbore treatment techniques. A small quantity of acid delivered to the desired position in the wellbore reacts with scale deposits or the formation. Acid may be circulated back and forth across the perforations or formation face.

Matrix acidizing is a type of stimulation to remove near-wellbore damage by injecting acid into the formation. The objective of matrix acidizing is to recover the original reservoir permeability or even create additional permeability (e.g. in carbonate formation). In sandstone formations, the acid attacks the clogging particles. Normally, sandstone formations are treated with hydrochloric/hydrofluoric (HCl/HF) mixtures. In carbonate formations (limestone and dolomite), the acid mainly attacks the matrix itself which creates secondary permeability. Hydrochloric acid is usually used in stimulation treatment of carbonate formations.

Hydraulic fracturing is stimulation treatment by creating fractures to connect the wellbore with the undamaged reservoir. Hydraulic fracturing is usually carried out in formations with low permeability whereas matrix acidizing is performed in medium to high permeability formations (k > 10 MD). Matrix acidizing treatment is regarded as inexpensive operation as compared to hydraulic fracturing in vertical wells but this is not true for horizontal wells.

2. FRACTURING FLUIDS AND ADDITIVES

The materials in this section were taken from [9], [6], [4], and [5].

The fracturing fluid is a critical component of the hydraulic fracturing treatment. Its main functions are to open the fracture and to transport proppants along the length of the fracture.

Consequently, the viscous properties of the fluid are usually considered the most important. However, successful hydraulic fracturing treatments require that the fluids have other special properties. In addition to exhibiting the proper viscosity in the fracture, they should break and clean up rapidly once the treatment is over, provide good fluid-loss control, exhibit low friction pressure during pumping and be as economical as is practical [5].

More than 90% of fracturing fluids are water-based according to [6]. The obvious reason is that aqueous fluids are cheaper and can provide control of a broad range of physical properties as a result of additives developed over the years.

The main purposes of additives for fracturing fluids are to enhance fracture creation and proppant-carrying capability and to minimise formation damage.

2.1. Properties of a Fracturing Fluid

The fracturing fluid must have certain physical and chemical properties to achieve successful stimulation.

- It should be compatible with the formation material.
- It should be compatible with the formation fluids.
- It should be capable of suspending proppants and transporting them deep into the fracture but should not carry it back during flow back.
- It should be capable, through its inherent viscosity, to develop the necessary fracture width to accept proppants or to allow deep acid penetration.
- It should be an efficient fluid (i.e., have a low fluid loss).
- It should be easy to remove from the formation.
- It should have low friction pressure.
- Preparation of the fluid should be simple and easy to perform in the field.
- It should be stable so that it will remain its viscosity throughout the treatment.
- The fracturing fluid should be cost-effective.

2.2. Types of Fracturing Fluids

Many different types of fluids have been developed to provide the properties described above because reservoirs to be stimulated vary in temperature, permeability, rock composition, and pore pressure [5].

Table-1 various types of hydraulic fracturing fluids and techniques

Type	Remark
Water base fluid	Predominant
Oil base fluid	Water sensitive; increase the hazard
Alcohol base fluid	Rare
Emulsion fluid	High pressure, low temperature
Foam base fluid	Low pressure, low temperature
Noncomplex gelled water fracture	Simple technology
Nitrogen foam fracture	Rapid cleanup
Complexed gelled water fracture	Often the best solution
Premixed gel concentrates	Improve process logistics
In situ precipitation technique	Reduce the concentration of the scale-forming ingredients

3. RESULTS AND DISCUSSION

3.1. Amplitude Sweep

In this series of measurements, the fracturing fluids were subjected to an angular frequency (ω) of 10 1/s based on [18]. The typical result from this measurement can be seen in Fig. 2 where amplitude strain γ (in the fraction) is plotted on the x-axis while both G' and G'' are plotted on the y-axis with both axes in a logarithmic scale. Later on, all amplitude strain values on the chart are presented in a fraction. It is noticeable from Fig. 2 that both curves are increasing from linear before decreasing1. This indicates an increasing proportion of the deformation energy (loss modulus G'') is being used up to change the structure before the final breakdown takes place [16]. Increasing values in G' curve could be a counter to maintain the structure from increasing proportion of the deformation energy.

It can be seen from Fig. 2, the G'' curve is considered linear until 100% strain (as a reminder: strain values on the chart are in a fraction; 1 in fraction equal to 100% in percentage). The G'' curve deviated to non-linear at strain approximately 118%. Based on those, it can be concluded for this fracturing fluid under measurement conditions the limit of the LVE range γ_L=118% below which the structure of the fracturing fluid is stable.

Further measurement was immediately performed for the same fracturing fluid presented in Fig. 2 with exactly the same setting configuration to get more information whether the limit of the LVE range was already exceeded. The results, gathered in Fig. 3, demonstrate that the limit of the LVE range has been exceeded since the curves were different. The 'increasing section' on the storage modulus curve after deformation does not appear in Fig. 3 as in Fig. 2. This could be because of the limit of the LVE range has been exceeded and the structure of the fracturing fluid sample has already been completely destroyed. This condition results in no counter act to maintain the structure from increasing proportion of the deformation energy.

In addition, it can be seen from Fig. 10 and 11 that this fracturing fluid has a gel character (G' > G") under measurement conditions. Here, the elastic behavior dominates over the viscous behavior [16].
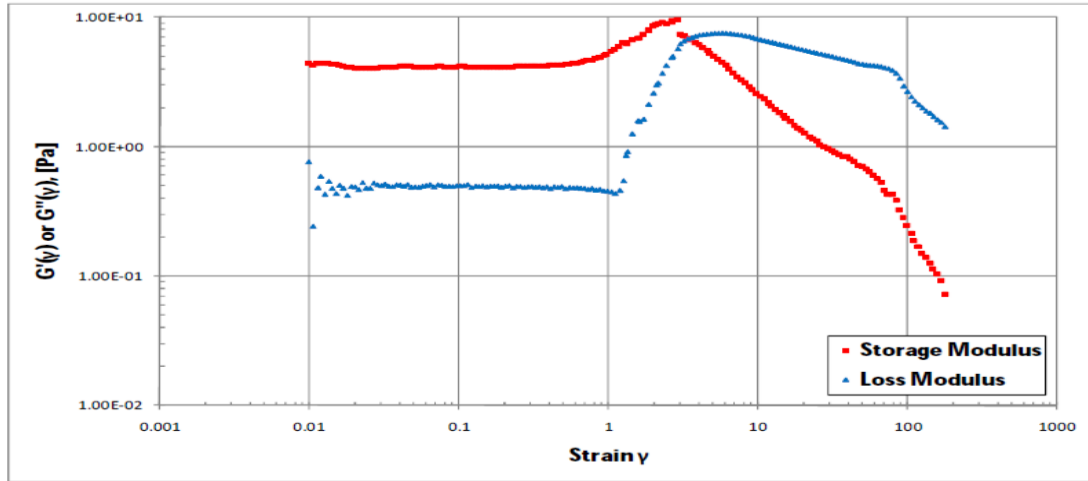

Figure 2 Typical G' (storage modulus) and G" (loss modulus) curves from amplitude sweep measurement. Here for fracturing fluid 2 at 20℃.
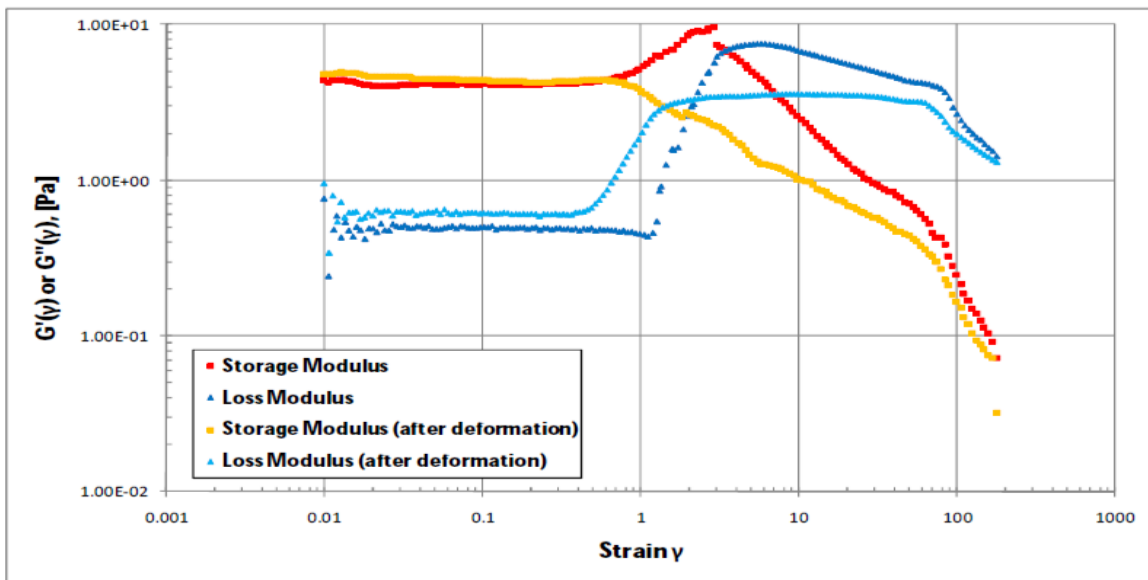

Figure 3 G' (storage modulus) and G" (loss modulus) curves from before and after deformation. Here for fracturing fluid 2 at 20℃.

3.2. Effect of Temperature and Polymer Concentration

The effect of temperature on limit of the LVE range for fracturing fluid 1 and 2 can be seen in Fig. 4 and 5, respectively. In Fig. 4 and 5, G' and G" are plotted versus strain at different temperature conditions. As the temperature increased, the limit of the LVE range also increased.

The effect of temperature and polymer concentration on the limit of LVE range may be better described in Fig. 6 and 7. In Fig. 6, the G' (γ) function is taken for the analysis for determining the limit of the LVE range. In this method, limit of the LVE range is strain value at which G' started increase continuously before decreasing. In the other hand, the G" (γ) function is taken for the analysis for determining the limit of the LVE range presented in Fig. 7. In this method, limit of the LVE range is strain value at which G" started increase or decrease continuously. The results depicted in Fig. 6 and 7 show that the limit of the LVE range increases when increasing the temperature but decreases when increasing the polymer concentration.

In the view of Fig. 6 and 7, it is noticeable that the plot of the limit of the LVE range (logarithmic scale) versus temperature (linear scale) in the semi-logarithmic diagram is a reasonably straight line.
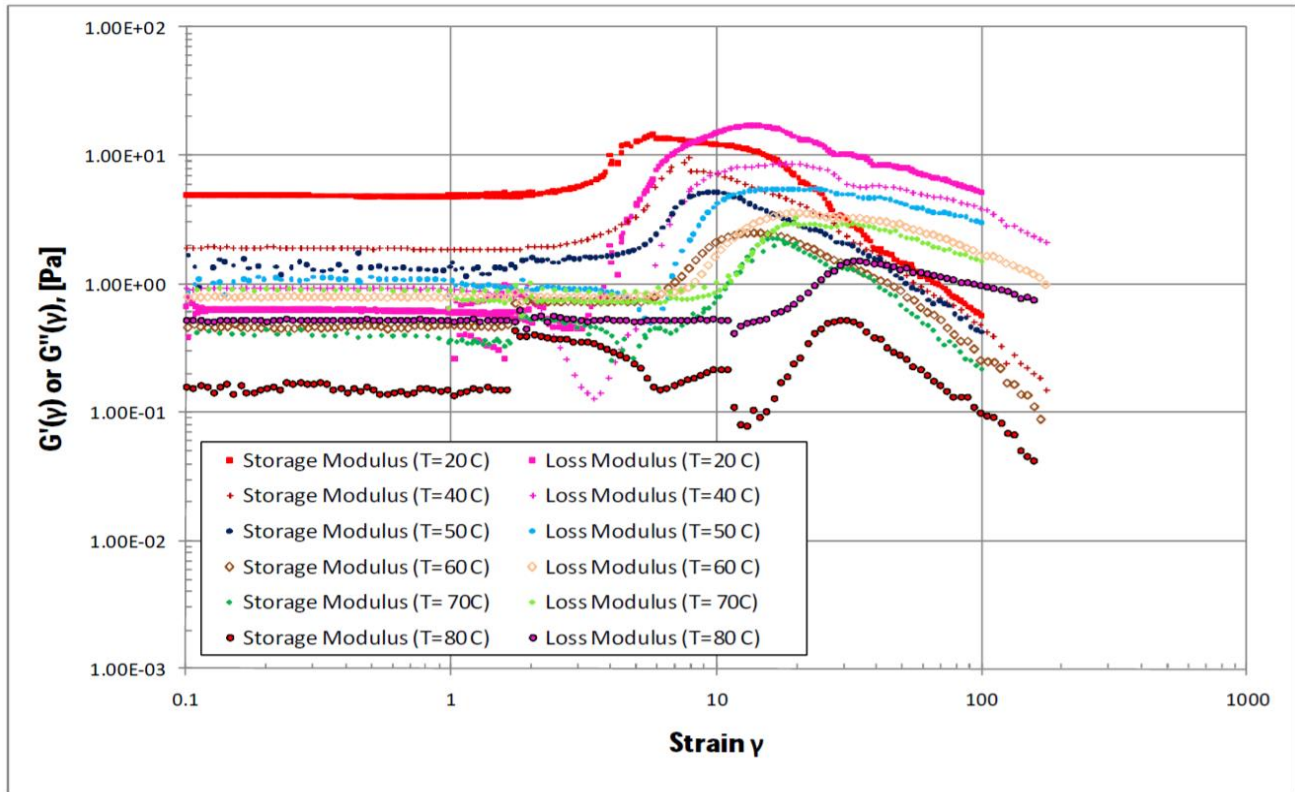
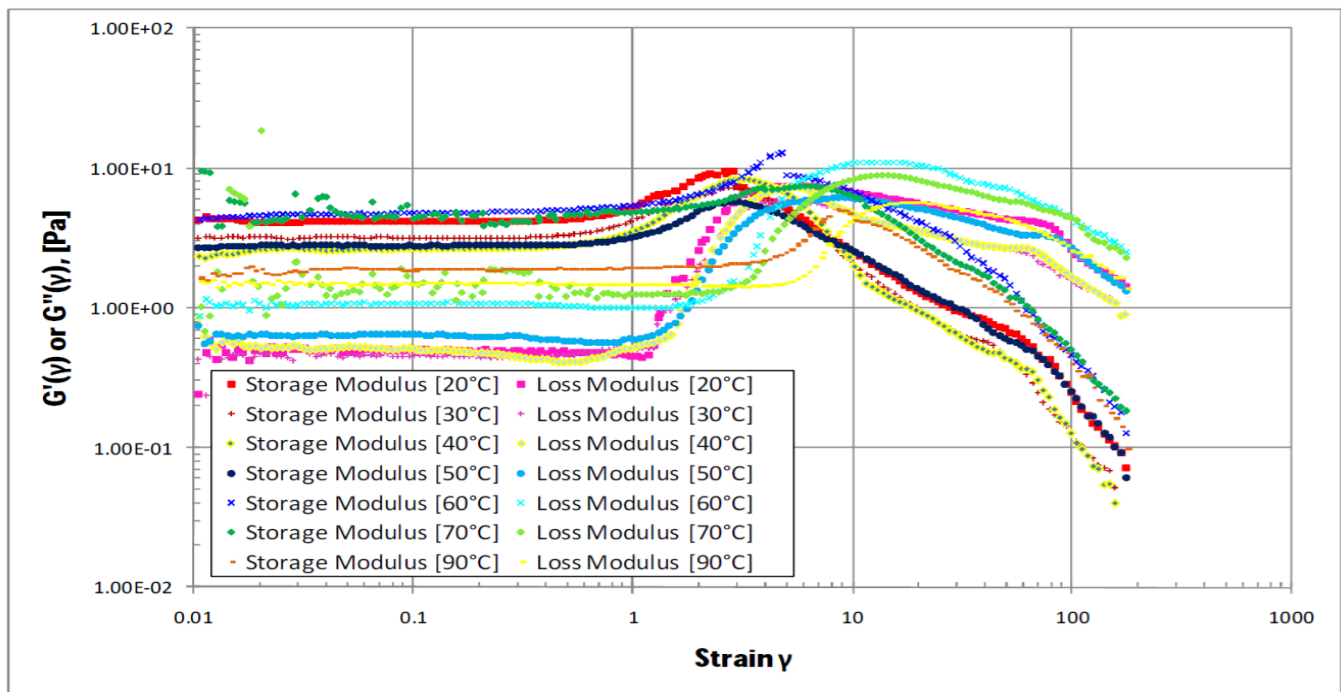Figure 4 G' and G'' versus strain for fracturing fluid 1 at different temperature

Figure 5 G' and G'' versus strain for fracturing fluid 2 at different temperature
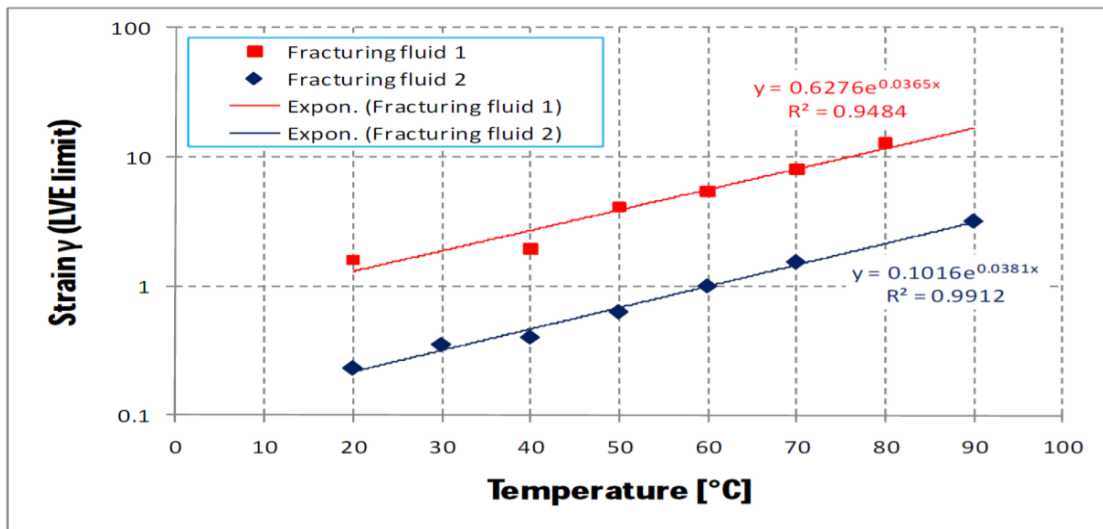
Figure 6 Limit of the LVE range and polymer concentration versus temperature. Here the G' (γ) function is taken for the analysis for determining the limit of the LVE range. The data fall approximately in straight line.
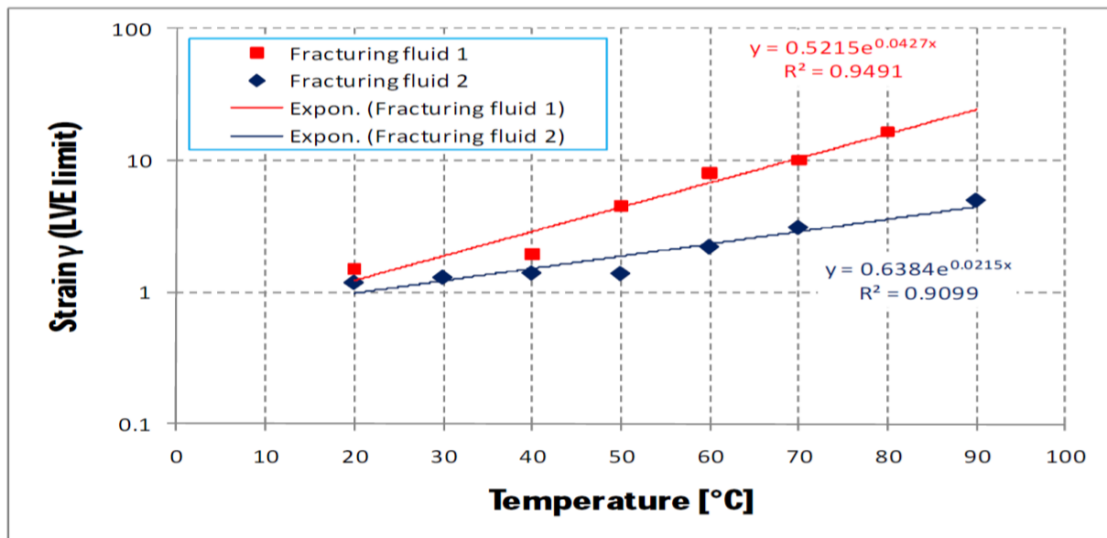

Figure 7 Limit of the LVE range and polymer concentration versus temperature. Here the G" (γ) function is taken for the analysis for determining the limit of the LVE range. The data fall approximately in straight line.

Observing Fig. 6 and 7, it is noticeable the dependence of the limit of the LVE range on temperature. The LVE limits for each fracturing fluid on further measurements were taken from the lowest value of the LVE limit from Fig. 6 and 7 at corresponding temperatures.

3.3. Time Test Oscillation

In this test, both the frequency and amplitude are set at a constant value in each individual test interval. The measuring temperature is also kept constant. In Fig. 8 the storage modulus (G'), loss modulus (G"), and tan δ are plotted versus time. In this series of measurements, fracturing fluid 1 was subjected to frequency 10 1/s at temperature 20ºc. This test consists of three intervals with different amplitude strain 1%, 5%, and 10% where time duration for each interval is 120, 120, and 60 minutes respectively.

Despite the noisy data for the first interval with amplitude strain 1%, it is obvious from Fig. 8 that this fracturing fluid sample has a time-independent or stable [12] structure with constant structure strength under test conditions where the elastic behavior dominates over viscous behavior (G' > G").
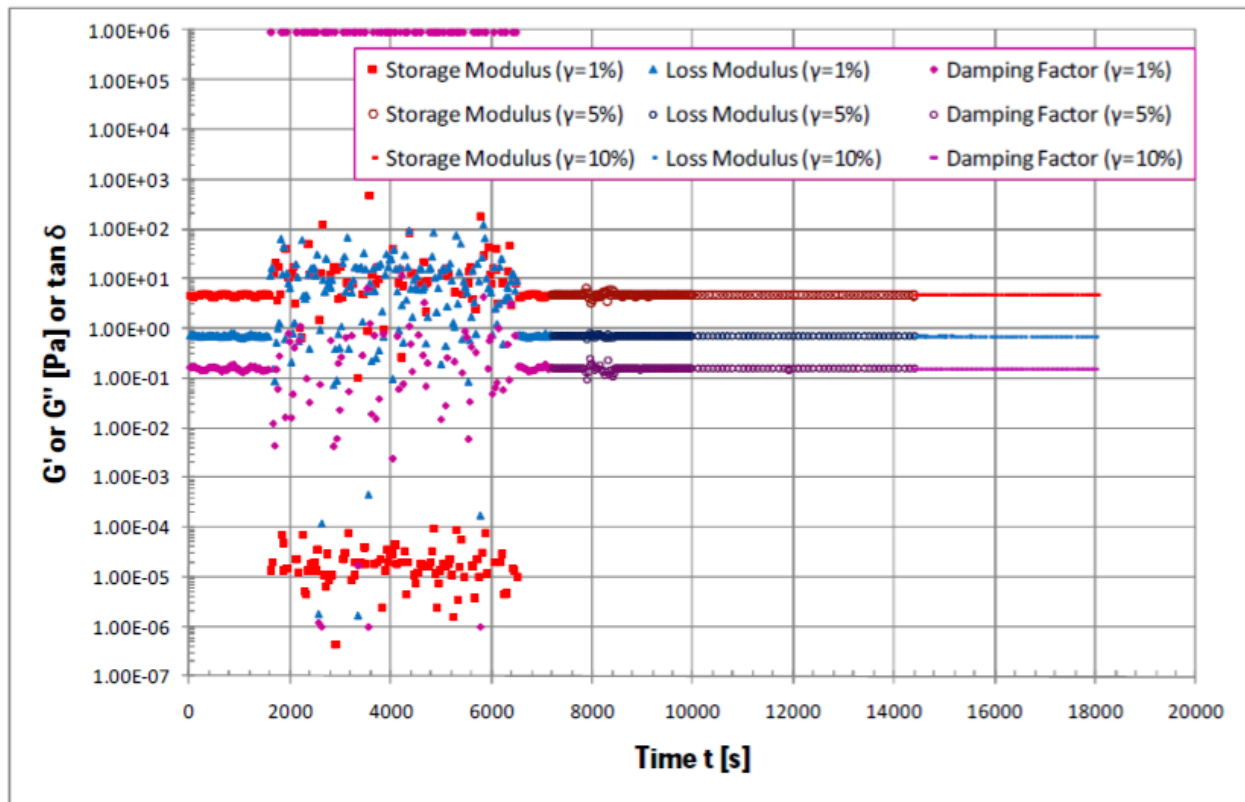
Figure 8 Time test oscillation result for fracturing fluid 1 at 20℃ with variation in amplitude strain (1%, 5%, and 10%). G', G", and tan δ versus time.

Time independent behaviour, despite variation in amplitude strain, also confirmed result regarding LVE range. It means the amplitude strain used in this test (1%, 5%, and 10%) are still within the LVE range.

3.4. Temperature Test Oscillation

Two measurements were conducted with fracturing fluid 1. In these measurements, the fracturing fluid samples were subjected to angular frequency 10 1/s and steady strain of 5% and 10%, respectively. As discussed earlier, the difference in amplitude strain should not affect the results as long as within the LVE range. The results gathered in Fig. 9, show that the curves are fit enough (as was expected) until temperature 74℃ after which the G' curves are different. This deviation could be due to the instability of the measuring environment.

Observing Fig. 9, the 'reaction temperature' at which the chemical reaction with crosslinking or hardening begins can be obtained. At this conditions, the G' curve shows minimum values [18]. In the view of Fig. 28, the reaction temperature for this fracturing fluid is approximately 74oC. With further heating, the G' (T) and G" (T) curves both increases. At higher temperatures, it can be expected to show a little softening (G' and G" curves decrease with slightly slope) due to heating up of the already hardened sample [18]. However, it cannot be shown here due to temperature limitation of the measuring device.

From Fig. 9, it can be seen that the fracturing fluid is in gel state (solid state, with G' > G") below 60℃. Above 60℃, the fracturing fluid is in sol state (liquid state, with G" > G'). The fracturing fluid shows sol state only until 78℃ above which it turns to a gel state. The temperature at which the G' and G" curves intersect is called the sol/gel transition temperature or gel temperature or gel point [18]. The sol/gel transition temperature for fracturing fluid 1 is approximately 78℃. At this temperature G' = G" or tan δ = 1. The melting temperature at approximately 60℃ is also noticeable in Fig. 9.

Another information from this measurement is temperature-dependent complex viscosity $|\eta^*(T)|$ of the fracturing fluid sample which is presented in Fig. 10. It can be seen from Fig. 10 that the viscosity minimum $|\eta^*min|$ of fracturing fluid 1 is approximately 5.5E-2 Pas at temperature 74℃.

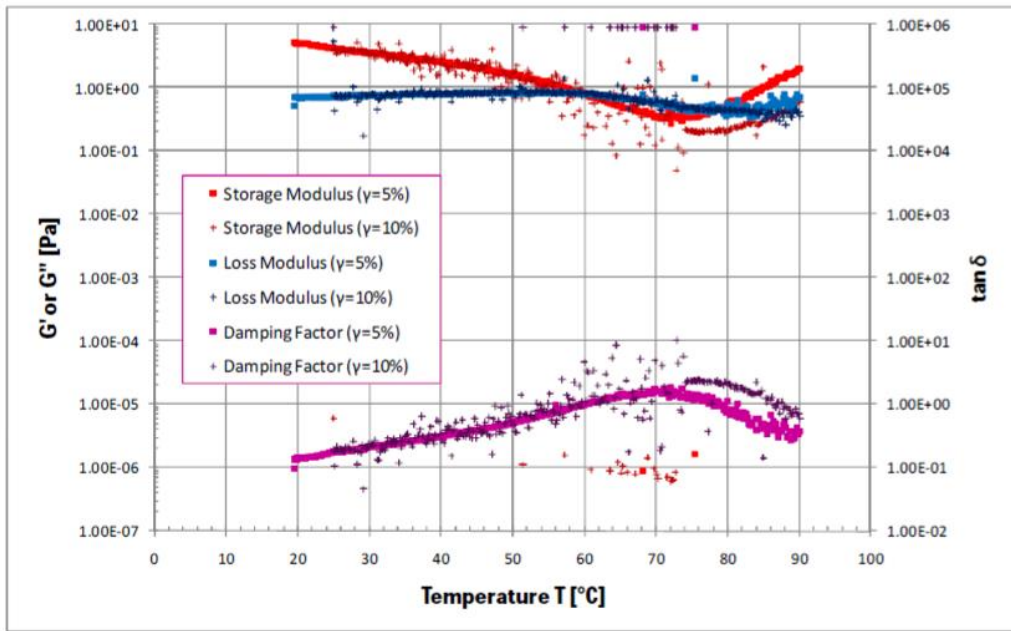Figure 9 Temperature test oscillation result for fracturing fluid 1 at angular frequency 10 1/s and amplitude strain of 5% and 10%. G', G", and tan δ versus temperature.
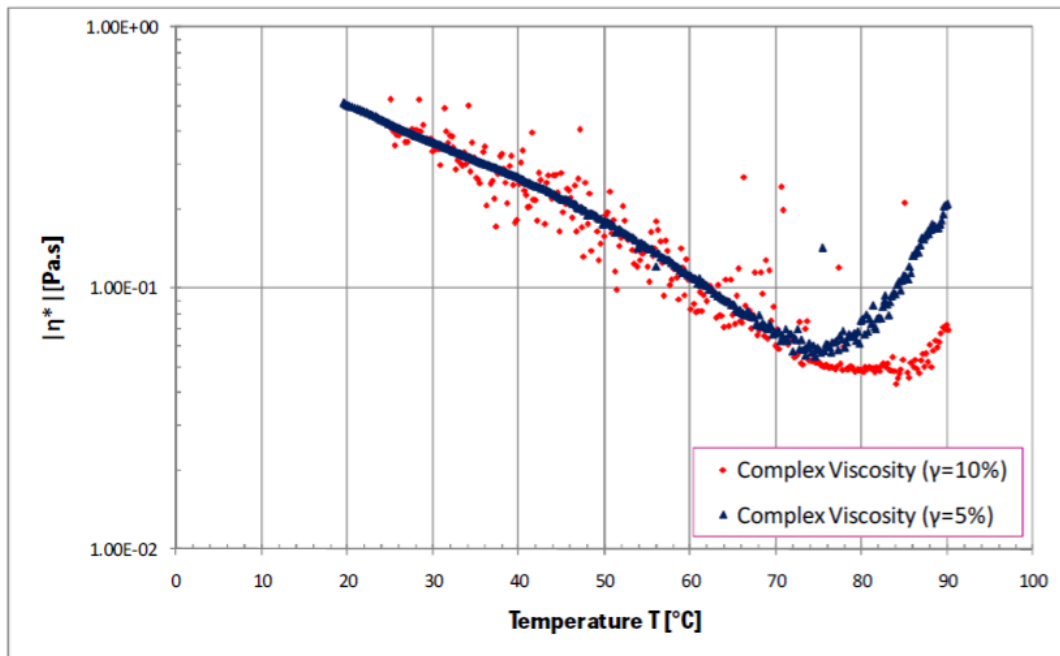

Figure 10 Complex viscosities versus temperature for fracturing fluid 1.

Temperature test oscillation measurements have also been performed for fracturing fluid 2 with two intervals where amplitude strains were 5% and 10%, respectively. In those measurements, the fracturing fluid samples were subjected to angular frequency 10 1/s. The results from those measurements gathered in Fig. 11; show that the curves are fit enough as was expected.

It can be seen from Fig. 11, there is no intersection between G' and G" curves or the sol/gel transition temperature. However, in the view of Fig. 11, the hardening could happen when G' displays sudden rise after 50℃ [20]. At this temperature, the G' curve shows minimum values. Further heating at a temperature above 65℃, it can be seen a little softening (G' and G" curves decrease with slightly slope) due to heating up of the already hardened sample [18].
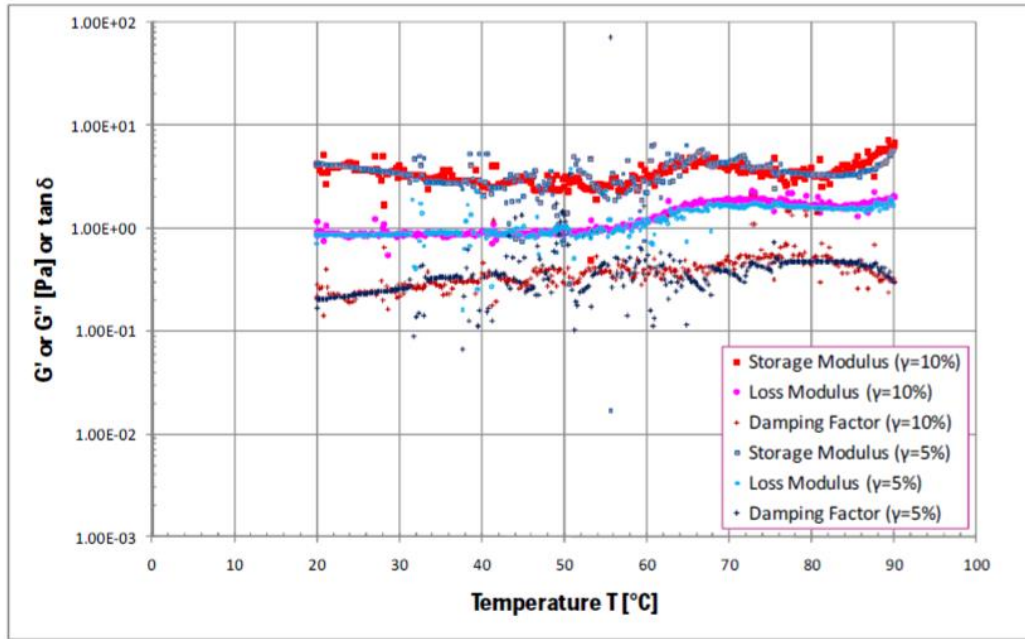
Figure 11 Temperature test oscillation result for fracturing fluid 2 at angular frequency 10 1/s and amplitude strain of 5% and 10%. G', G'', and tan δ versus temperature.

In Fig. 12, the complex viscosity is plotted versus temperature. It can be observed from Fig. 12 that the viscosity minimum $|\eta^*min|$ of fracturing fluid 2 is approximately 2.4E-1 Pas at temperature 55℃.
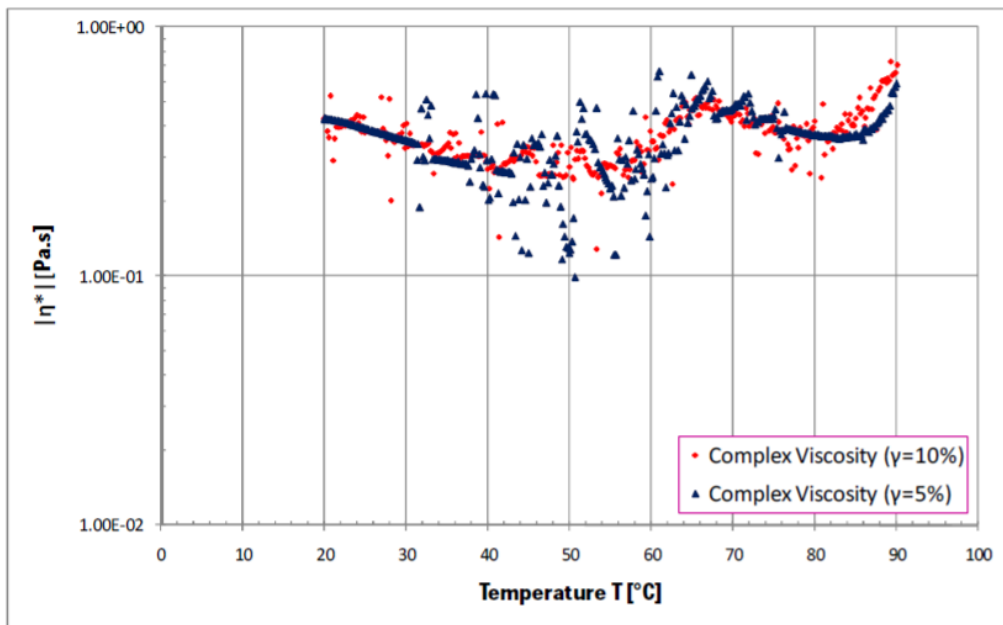

Figure 12 Complex viscosities versus temperature for fracturing fluid 2.

Nevertheless, it is important to mention the limitations and conditions that might affect the experiment. The experiments were performed in 'open system' that could be affected by outside temperature. It is suggested to perform the experiment in 'close system' if possible.

The fracturing fluids in this experiment might undergo chemical modification with time. One of these chemical instabilities is known as syneresis. Syneresis causes shrinkage in gel volume and consequently, water is expelled from the gel structure [21]. This could result in non-homogeneous in the sample mixture. There were also lumps observed in the sample.

CONCLUSION

Oscillatory measurements have been performed to investigate the behavior of the rheological properties of the borate cross-linked fracturing fluids and the possible relationship among them. The main results are as follows:

- The amplitude sweep measurements show the temperature-dependence of the LVE limit. The plot of the LVE limit versus temperature in the semi-logarithmic diagram is a reasonably straight line.
- The storage modulus and loss modulus are independent of amplitude strain at LVE region.
- It was demonstrated that frequency sweep can differentiate a number of specific regions of the fracturing fluids in the viscoelastic spectrum (the viscous or terminal region, the transition to flow region, the rubbery or plateau region, the leathery or higher transition crossover region, and the glassy region).
- The flow-point frequency of the fracturing fluids is dependent on temperature. It increases exponentially with temperature.
- The gel points (time and temperature) are observable using time and temperature test oscillation.
- Additional information on the structural character of fracturing fluid can be obtained from G' and G" curves. It means that viscosity is inadequate in describing fracturing fluids.

REFERENCES:

[1] Bale, A., Larsen, L., Barton, D. T., and Buchanan, A. 2001. Propped Fracturing as a Tool for Prevention and Removal of Formation Damage. Paper SPE 68913 presented at the SPE European Formation Damage Conference, The Hague, The Netherlands, 21-22 May.

[2] Barnes, H. A. 2000. A handbook of elementary rheology. Aberystwyth: Univ. of Wales, Institute of Non-Newtonian Fluid Mechanics.

[3] Barnes, H. A., Hutton, J. F., and Walters, K. 1989. An introduction to rheology. Amsterdam: Elsevier.

[4] Economides, M. J. 2007. Modern Fracturing Enhancing Natural Gas Production. Houston: Energy Tribune Publishing Inc.

[5] Economides, M. J. and Nolte, K. G. 2000. Reservoir stimulation. Chichester: Wiley.

[6] Fink, J. K. 2003. Oil field chemicals. Amsterdam: Gulf Professional Publ.

[7] Friehauf, K. E. and Sharma, M. M. 2009. Fluid Selection for Energized Hydraulic Fractures. Paper SPE 124361 presented at the SPE Annual Technical Conference and Exhibition, New Orleans, Louisiana, USA, 4-7 October.

[8] Friehauf, K. E., Suri, A., and Sharma, M. M. 2009. A Simple and Accurate Model for Well Productivity for Hydraulically Fractured Wells. Paper SPE 119264 presented at the SPE Hydraulic Fracturing Technology Conference, The Woodlands, Texas, USA, 19- 21 January.

[9] Gidley, J. L., Holditch, S. A., Nierode, D. E., and Veatch Jr., R. W. 1989. Recent advances in hydraulic fracturing. Monograph Series. New York: SPE.

[10] Goel, N., Willingham, J. D., Shah, S. N., and Lord, D. L. 1997. A Comparative Study of Borate-Crosslinked Gel Rheology Using Laboratory and Field Scale Fracturing Simulations. Paper SPE 38618 presented at the SPE Annual Technical Conference and Exhibition, San Antonio, Texas, USA, 5-8 October.

[11] Guo, B., Lyons, W. C., and Ghalambor, A. 2007. Petroleum production engineering: a computer-assisted approach. Amsterdam: Elsevier.

[12] Guo, B., Sun, K., and Ghalambor, A. 2008. Well productivity handbook: vertical, fractured, horizontal, multilateral, and intelligent wells. Houston, Tex.: Gulf Publ. Co.

[13] Harris, P. C. 1993. Chemistry and Rheology of Borate-Crosslinked Fluids at Temperatures to 300°F. SPE Journal of Petroleum Technology, 45(3), 264-269.

[14] Harris, P. C. and Heath, S. J. 1998. Rheological Properties of Low-Gel-Loading Borate Fracture Gels. SPE Production & Operations, 13(4), 230-235.

[15] Huang, T. and Crews, J. B. 2007. Nanotechnology Applications in Viscoelastic Surfactant Stimulation Fluids. Paper SPE 107728 presented at the European Formation Damage Conference, Scheveningen, The Netherlands, and 30 May-1 June.

[16] Kesavan, S., Prud'homme, R. K., and Parris, M. D. 1993. Crosslinked Borate HPG Equilibria and Rheological Characterization. Paper SPE 25205 presented at the SPE International Symposium on Oilfield Chemistry, New Orleans, LA, USA, and 2-5 March.

[17] Mezger, T. G. 2006. The rheology handbook: for users of rotational and oscillatory rheometers. Hannover: Vincentz Verlag.

[18] Mezger, T. G. 2002. The rheology handbook: for users of rotational and oscillatory rheometers. Hannover: Vincentz Verlag.

[19] Penny, G. S., Pursley, J. T., and Holcomb, D. 2005. The Application of Microemulsion Additives in Drilling and Stimulation Results in Enhanced Gas Production. Paper SPE 94274 presented at the SPE Production Operations Symposium, Oklahoma City, OK, USA, and 17-19 April.

[20] Romero-Zeron, L., Manalo, F., and Kantzas, A. 2008. Characterization of Crosslinked Gel Kinetics and Gel Strength by Use of NMR. SPE Reservoir Evaluation & Engineering, 11(3), 439-453.

[21] Romero-Zeron, L., Manalo, F., and Kantzas, A. 2004. Characterization of Crosslinked Gel Kinetics and Gel Strength Using NMR. Paper SPE 86548 presented at the SPE International Symposium and Exhibition on Formation Damage Control, Lafayette, Louisiana, USA, and 18-20 February.

[22] Shah, S. N., Lord, D. L., and Rao, B. N. 1997. Borate-Crosslinked Fluid Rheology under Various pH, Temperature, and Shear History Conditions. Paper SPE 37487 presented at the SPE Production Operations Symposium, Oklahoma City, Oklahoma, USA, and 9-11 March.

[23] Shah, S. N., Lord, D. L., and Tan, H. C. 1992. Recent Advances in the Fluid Mechanics and Rheology of Fracturing Fluids. Paper SPE 22391 presented at the International Meeting on Petroleum Engineering, Beijing, China, and 24-27 March.

[24] Sinclair, A. R. 1970. Rheology of Viscous Fracturing Fluids. SPE Journal of Petroleum Technology, 22(6), 711-719.

[25] Walters, H. G., Morgan, R. G., and Harris, P. C. 2001. Kinetic Rheology of Hydraulic Fracturing Fluids. Paper SPE 71660 presented at the SPE Annual Technical Conference and Exhibition, New Orleans, Louisiana, USA, 30 September-3 October.

[26] Young, N. W. G., Williams, P. A., Meadows, J., and Allen, E. 1998. A Promising Hydrophobicaly-Modified Guar for Completion Applications. Paper SPE 39700 presented at the SPE/DOE Improved Oil Recovery Symposium, Tulsa, Oklahoma, 19- 22 April.

[27] Zolotukhin, A., Risnes, R., and Mishchenko, I. T. 2005. Performance of Oil and Gas Wells. Stavanger: University of Stavanger.